PCCP

Accepted Manuscript

ROYAL SOCIETY OF CHEMISTRY

www.rsc.org/pccp

Manuscript submitted to PCCP

Crystal-plane-dependent Metal-Support Interaction in Au/TiO_2

Lichen Liu,[a] Chengyan Ge,[a] Weixin Zou,[a] Xianrui Gu,[a] Fei Gao,[b]* Lin Dong [a,b]*

[a] Key Laboratory of Mesoscopic Chemistry of Ministry of Education, School of Chemistry and Chemical Engineering, Nanjing University, Nanjing 210093, PR China

[b] Jiangsu Key Laboratory of Vehicle Emissions Control, Center of Modern Analysis, Nanjing University, Nanjing 210093, PR China

Abstract

Metal-support interaction in between Au and TiO_2 are studies based on Au/TiO_2 catalysts with different TiO_2 crystal planes exposed. With *ex situ* XPS, TEM and *in situ* DRIFTS, we have investigated the crystal-plane-dependent metal-support interaction effects on the physiochemical properties of Au/TiO_2 catalysts. Based on the structural characterizations and spectroscopic results, we can observe chemical oscillations (including the electronic structures of Au nanoparticles and the interaction between Au/TiO_2 catalysts and CO molecules) during alternate H_2 and O_2 pre-treatments. Their variation tendencies of oscillations are greatly dependent on the crystal planes of TiO_2 and the pre-treatment temperature. Furthermore, their surface and electronic changes after H_2 and O_2 pre-treatments can be well correlated with their catalytic activities in CO oxidation. Electron-transfer processes across the Au-TiO_2 interface are proved to be the origin accounting for their changes after H_2 and O_2 pre-treatments. The different electronic structures of different TiO_2 crystal planes should have relationships with the crystal-plane-dependent metal-support interaction effects in Au/TiO_2.

Keywords: Metal-support interaction, Au/TiO_2, Crystal-plane effect, CO oxidation, *Ex situ* XPS, *In situ* DRIFTS

Metal nanoparticles (NPs) supported on metal oxides are widely used heterogeneous catalysts in many industrial applications including chemical, food, pharmaceutical, environmental and petrochemical industries.[1] The superior catalytic performances are usually related with the metal-support interaction between metal NPs and metal oxide supports.[2] The classic strong metal-support interaction (SMSI) effect was firstly revealed from the interaction between Group VIII metals and TiO_2.[3] Under reductive atmosphere (usually H_2) at high temperature, electrons will transfer from TiO_2 support to metal NPs, leading to the encapsulation of metal NPs by thin shells of TiO_2.[4] Associated with these electronic and geometric changes, the chemisorption behaviors and catalytic properties are affected.[5,6] On the other hand, the SMSI effect between the metal NPs and metal oxide supports can be tuned through tuning the electronic structures of the metal oxide supports.[7,8] Based on numerous works, SMSI is proved to play a crucial role in catalytic properties of metal/oxide catalysts.

However, previous studies on SMSI are mainly focused on Group VIII metals (Pt, Pd, Rh etc.), while few works have discussed the metal-support interaction of Au NPs supported on oxides. Au NPs supported on metal oxides have shown excellent catalytic performances in many reactions.[9,10] And the fantastic activities of Au NPs have been proved to be related with interaction Au NPs and the support.[11,12] Goodman has proposed that Au/TiO_2 maybe another example of SMSI through comparing the similarities and discrepancies Au/TiO_2 and Group VIII metals/TiO_2 on their catalytic behaviors.[13] Takeda *et al.* have studied the dynamic changes of Au/TiO_2 catalysts by *in situ* environmental TEM under reaction atmosphere. Au NPs can be encapsulated by TiO_{2-x} shells under O_2 atmosphere and electron irradiation.[14] The electron transfer from Au NPs to TiO_2 support also has been *in situ* observed when Au/TiO_2 is exposed to O_2, which is different with the situation in H_2-pretreated Pt/TiO_2.[15,16] These works imply that SMSI should also exist in Au/TiO_2 although it may work in different mechanism. So, studying the metal-support interaction in Au/TiO_2 can provide further insights into the catalytic properties.

What's more, for the classic SMSI model, the interface between metal and oxide support is thought to be the reaction zone.[17,18] The surface structures and electronic structures of the metal-oxide interface will show significant effects on the SMSI between metal and oxide. As we know, the catalytic activities of metal NPs are greatly dependent on the crystal planes of oxide

supports.[19-21] However, to the best of our knowledge, this crystal-plane effect on the metal-support interaction has not been studied, which is probably due to the difficulties in obtaining single oxide crystals with different crystal plane exposed. Considering their different surface structures and electronic structures of different crystal planes of metal oxides,[22] it will be meaningful to study the crystal-plane effect on metal-support interaction.

In this work, we have prepared TiO_2 nanocrystals with different crystal planes ({100}, {101} and {001}) exposed as support of Au NPs to study the crystal-plane effect on the metal-support interaction in Au/TiO_2 catalysts. With the help of *ex situ* XPS and *in situ* DRIFTS, the dynamic changes of Au NPs supported on different TiO_2 crystal planes under reaction atmosphere are investigated. We have found some similar phenomenon like traditional SMSI in as-prepared Au/TiO_2 catalysts as well as some differences. More interestingly, the results show that the responses of Au/TiO_2 catalysts to different atmosphere at different temperature will vary with the crystal planes of TiO_2 nanocrystals. This work may provide some new insights into the Au-TiO_2 interaction and the working mechanism, especially the interfacial interaction in reaction atmosphere.

TiO_2 nanocrystals with different crystal planes exposed are synthesized according to our recent works through an anion-assisted method.[23] The as-prepared TiO_2 nanocrystals show typical XRD patterns of anatase TiO_2 without other peaks. These TiO_2 nanocrystals show regular shapes and similar sizes. Based on the TEM and HRTEM images, their dominant crystal facets are identified to {100}, {101} and {001} facets, and the percentages of specific crystal planes are as high as ca. 80%, which suggests that they are ideal model supports. Structural characterizations on the Au/TiO_2 catalysts with different TiO_2 crystal planes exposed can also be found in our recent work.[24] Au NPs are loaded on these TiO_2 nanocrystals through deposition-precipitation method. We can figure out that Au NPs (average size is ca. 3.6 nm) are located on specific crystal facets of TiO_2 nanocrystals. Therefore, these Au/TiO_2 catalysts can be used as model catalysts to investigate the crystal-plane-dependent metal-support interaction effect.

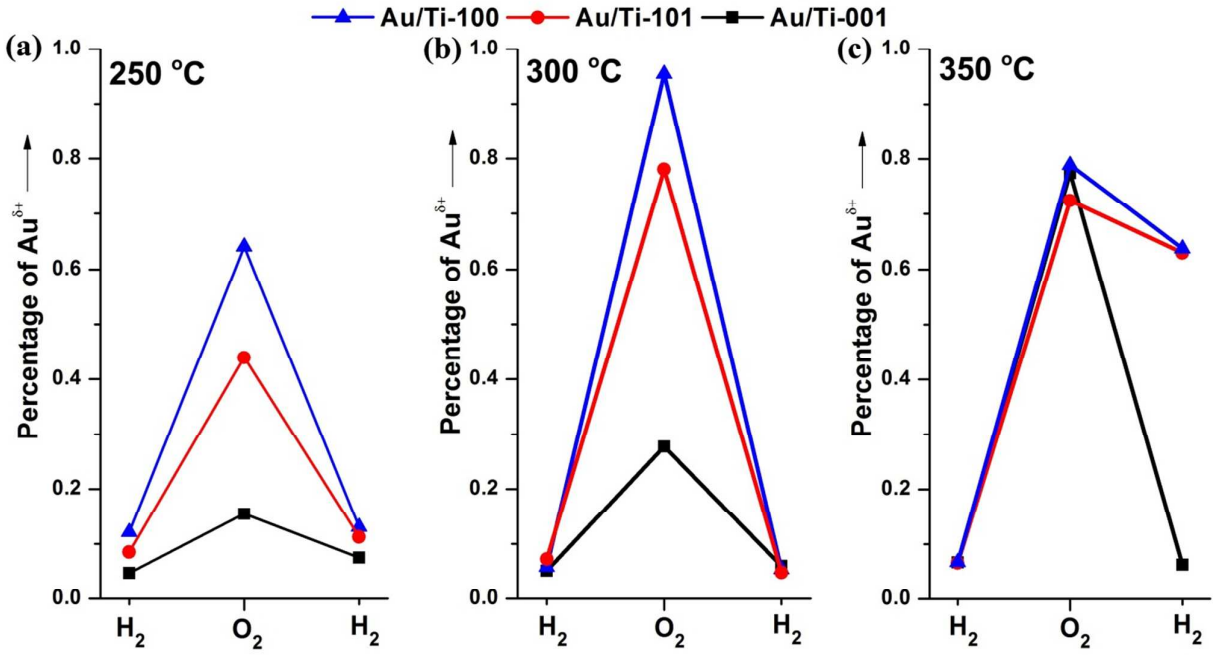

Fig. 1. Percentage of $Au^{\delta+}$ calculated from the *ex situ* XPS spectra in different Au/TiO_2 catalysts at 250 °C (a), 300 °C (b) and 350 °C (c) after pre-treatments under H_2 or O_2.

According to previous works, SMSI is usually induced by the pre-treatments of reductive or oxidative atmosphere at high temperature. The interfacial electron transfer will be caused by these pre-treatments and will further have great influences on the electronic and surface structures of the catalysts. Firstly, we use *ex situ* XPS to investigate the interfacial electron transfer across the Au-TiO_2 interface during the pre-treatments at high temperature. The XPS spectra of Au 4f region are shown in **Fig. S1-S3**. In order to clarify the dynamic changes of Au NPs during the alternate pre-treatments, the percentages of cationic Au species (denoted as $Au^{\delta+}$) are calculated according to the fitting results.[25,26] As displayed in **Fig. 1**, the chemical states of Au will change with the atmosphere. The percentages of $Au^{\delta+}$ in three Au/TiO_2 samples show different variation tendencies under H_2 and O_2 atmosphere. For Au/Ti-100 and Au/Ti-101, the percentages of $Au^{\delta+}$ are very sensitive to the atmosphere at 250 °C and 300 °C (as shown in **Fig. 1a-b**). When they are pre-treated with H_2, the percentages of $Au^{\delta+}$ will decrease compared with those under N_2 atmosphere. When the atmosphere is shifted to O_2, the percentages of $Au^{\delta+}$ are dramatically improved. Therefore, a chemical oscillation of chemical states of Au will appear. However, the variation tendency will

change for Au/Ti-001. At the relative low temperature (250 ^{o}C and 300 ^{o}C), Au/Ti-001 still shows insensitive to the atmosphere. The percentages of $Au^{\delta+}$ are kept below 10% no matter pre-treated by H_2 or O_2. When the pre-treatment temperature increases to 350 ^{o}C, the percentage of $Au^{\delta+}$ can be significantly improved by O_2 oxidation. Furthermore, the content of $Au^{\delta+}$ will subsequently decrease after H_2 treatment. Thus, an oscillation of chemical states of Au can be also observed in Au/Ti-001 if the temperature is high enough, which may be caused by the high energy barrier for charge transfer between Au NPs and TiO_2 {001} planes. Moreover, the high temperature also has a dramatic effect on Au/Ti-100 and Au/Ti-101. As displayed in **Fig. 1c**, the percentages of $Au^{\delta+}$ in Au/Ti-100 and Au/Ti-101 are still very high after the second H_2 pre-treatment, which shows great contrast with their dramatic variation at 250 ^{o}C and 300 ^{o}C. The oscillation of chemical states of Au should be originated from the charge transfer between Au NPs and TiO_2 support under reductive or oxidative atmosphere. During H_2 pre-treatment, electrons will transfer from TiO_2 to Au NPs, resulting in the decrease of percentages of $Au^{\delta+}$. While during O_2 pre-treatment, electrons will flow from the Au NPs to TiO_2 support, leading to the increase of percentages of $Au^{\delta+}$.[27,28] The charge transfer processes should have relationships with the electronic properties of different TiO_2 crystal planes, therefore three Au/TiO_2 catalysts show different variation tendencies during the alternate H_2 and O_2 pre-treatments.

In order to figure out the structural changes in these samples during the pre-treatment in O_2, we use TEM to study them after O_2 pre-treatment. When three Au/TiO_2 samples are pretreated in O_2 at 250 ^{o}C and 300 ^{o}C, no obvious morphological changes can be found (as shown in **Fig. S4-S6**). Au NPs are still located on corresponding crystal planes of TiO_2 without obvious growth of particle size. However, Au NPs will be encapsulated by a TiO_2 shell after O_2 treatment at 350 ^{o}C (**Fig. 2a-d**). This encapsulation may be caused by the strong interaction between Au and TiO_2 at high temperature in O_2 atmosphere.[14,29] Driven by the oxidative atmosphere at high temperature, electrons will flow to TiO_2 support, forming TiO_{2-x} at the Au-TiO_2 interface.[15] Then TiO_{2-x} will crawl along Au NPs, resulting in the encapsulation of Au NPs by TiO_2. Due to the encapsulation, the percentage of $Au^{\delta+}$ species cannot fall back after H_2 treatment. Interestingly, this encapsulation is not observed in Au/Ti-001 (**Fig. 2e-f**). No TiO_2 can be found at the Au-{001} plane interface, indicating that TiO_2 will not crawl along Au NPs in O_2 atmosphere at 350 ^{o}C. Therefore, the $Au^{\delta+}$ species in Au/Ti-001

can be reduced by H_2 at 350 ^oC. Specially, the mechanism of encapsulation of Au NPs observed in our work is different from classic SMSI models. The encapsulation of Au NPs in our work is induced by O_2 pre-treatment while the encapsulation of Group VIII metal NPs in previous works is induced by H_2 pre-treatment.[30,31] Nevertheless, these Au NPs are still covered by TiO_{2-x} shells after H_2 treatment under 350 ^oC (see **Fig. S7**), suggesting that the encapsulation is irreversible, which is also different from the classic SMSI. This large discrepancy may be caused by the different electronic structure of Au compared with Group VIII metals.[32] However, the encapsulation of Au NPs may also be caused by the surface reconstruction of TiO_2 support. At high temperature, surface structures of metal oxides will be reconstructed, which may also lead to the encapsulation of metal NPs.[31,32] Similar encapsulation phenomenon of Au NPs is also found in some other systems which are also induced by high-temperature treatment under O_2 atmosphere.[29,32-37] Further investigations need to be done to figure out the encapsulation mechanism of Au NPs supported on TiO_2.

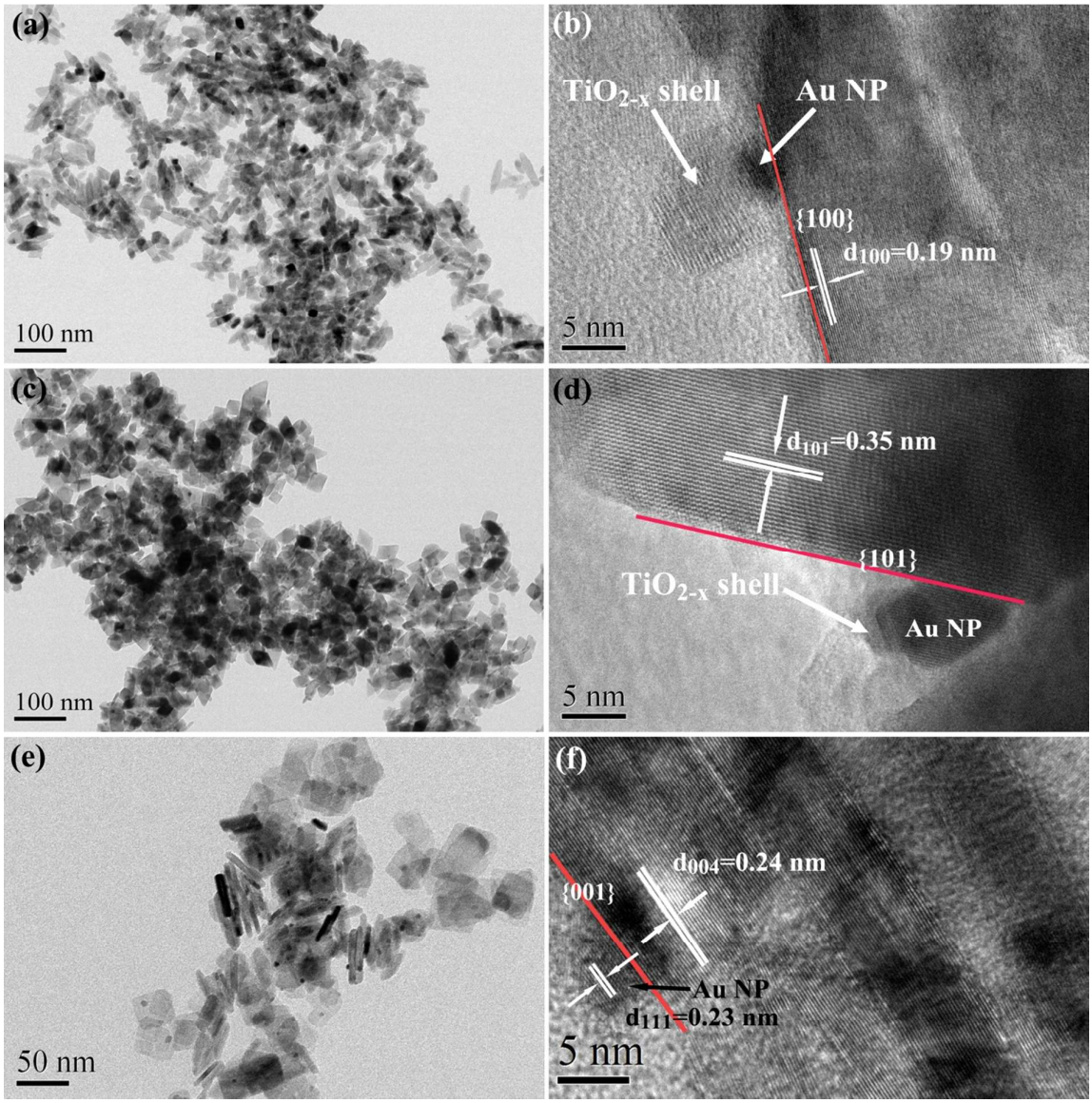

Fig. 2. TEM images and HRTEM images of Au/Ti-100 (a, b), Au/Ti-101 (c, d) and Au/Ti-001 (e, f) after pretreating with O_2 at 350 ^oC.

Based on the *ex situ* XPS and TEM results, we can understand the In Au/Ti-100 and Au/Ti-101, the electron transfer between Au NPs and TiO_2 is facilitated due to the stronger interactions between Au NPs and {100} planes and {101} planes. Therefore, the percentages of $Au^{\delta+}$ will show evident oscillation during the alternate pre-treatments at 250 ^oC and 300 ^oC. As to Au/Ti-001, the charge transfer across the Au-TiO_2 interface is not propitious, which makes the percentage of $Au^{\delta+}$ stable at 250 ^oC and 300 ^oC during pre-treatment processes. However, the situation will change when the pre-treatment temperature is increased to 350 ^oC. In Au/Ti-100 and Au/Ti-101, Au NPs will be

encapsulated by TiO_{2-x} shells, which may hinder the electron transfer process between Au NPs and TiO_2.[38,39] As a consequence, the percentages of $Au^{\delta+}$ keep stable after O_2 pre-treatment at 350 ^oC. For Au/Ti-001, the encapsulation is not occurred. What's more, the electron-transfer process between Au NPs and {001} facets is facilitated by the high temperature, which causes the obvious oscillation of $Au^{\delta+}$ percentage.

With the help of *ex situ* XPS and TEM, we have studied the crystal-plane effects on the electron-transfer process between Au NPs and TiO_2 supports. Then, *in situ* DRIFTS are used to study the effects of H_2 and O_2 pre-treatments on the interactions between CO molecules and Au NPs supported on different TiO_2 crystal planes. At first, the effects of H_2 pre-treatments are discussed. As shown in **Fig. S8-S10**, two peaks appear in all the three Au/TiO_2 catalysts after N_2 pretreatment. They can be ascribed to $Au^{\delta+}$-CO (2110-2120 cm^{-1}) and Au^0-CO (2070-2080 cm^{-1}), respectively.[38,39] Notably, the peaks corresponding to $Au^{\delta+}$-CO will disappear and new adsorption signals (2063-2067 cm^{-1}) can be observed after H_2 reduction. The new adsorption peaks are corresponding to $Au^{\delta-}$-CO, which should result from the CO adsorbed on negative charged Au NPs.[40] The intensity of Au^0-CO will decrease with the increase of temperature. *Ex situ* XPS have proved that electrons will transfer from TiO_2 to Au NPs during H_2 pre-treatment, leading to the accumulation of negative charge in Au NPs. After pre-treated by H_2 at higher temperature, more electrons will transfer to Au NPs, which is not favoured for the adsorption of CO.[29,40] For negative charged Au NPs, CO adsorption is not facilitated, which have already been reported in some previous works.[41,42] For Au/Ti-100 and Au/Ti-101, the adsorption of CO is very weak after high temperature reduction. For Au/Ti-001, the peak corresponding to Au^{δ}-CO is still fairly strong, implying that the amounts of negative charges accumulated in Au NPs may vary with the crystal planes of TiO_2. Under the H_2 pre-treatment at same temperature, more electrons may flow to Au NPs on {100} and {101} planes than those on {001} planes.

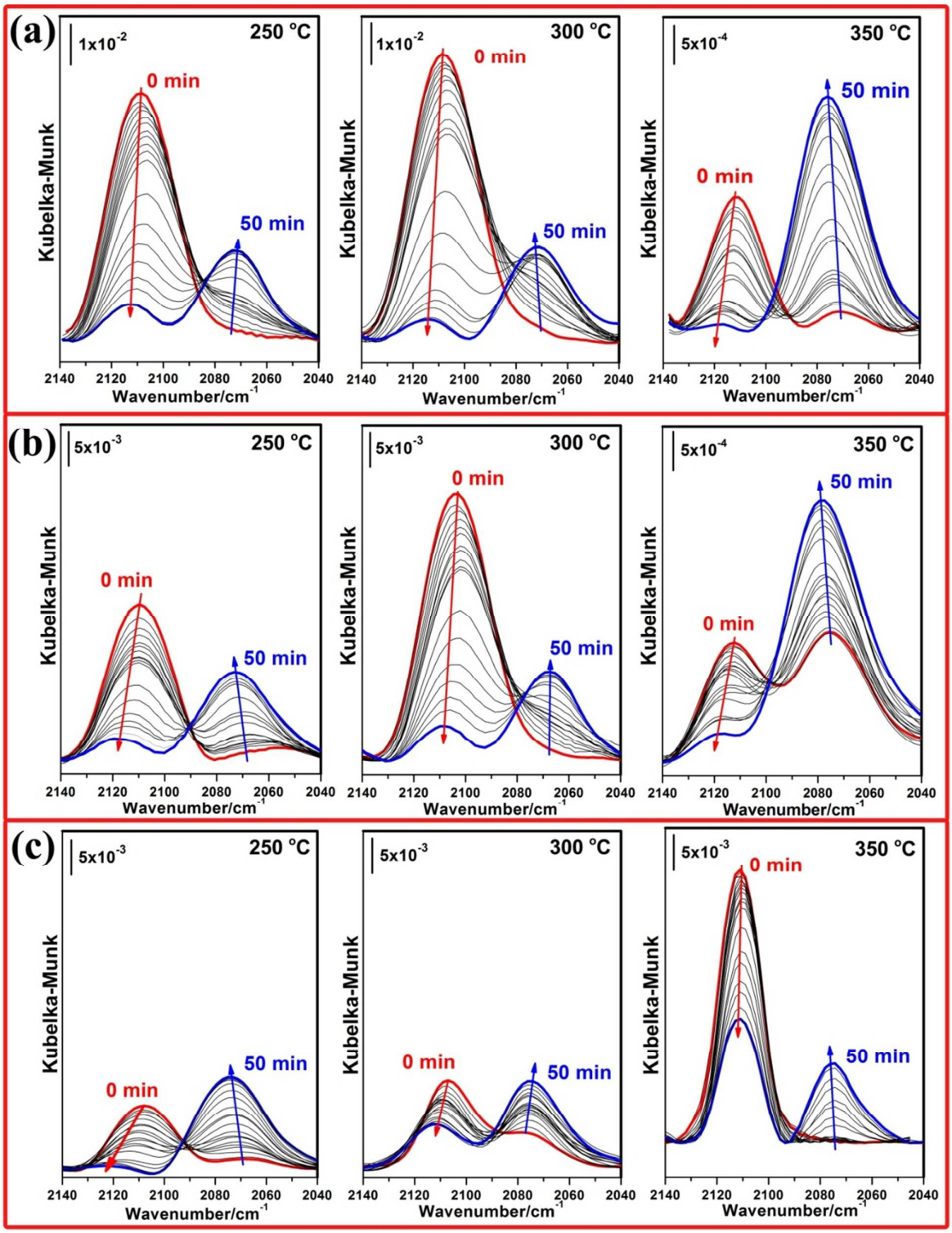

Fig. 3. *In situ* DRIFTS of CO adsorption on Au/Ti-100 (a), Au/Ti-101 (b) and Au/Ti-001 (c) after pretreated with O_2 at 250 ^oC, 300 ^oC and 350 ^oC. The intensity scale bar is put at the top left corner of each figure.

What's more, we also track the influences of O_2 pretreatments on the adsorption properties of Au/TiO_2 catalysts to CO molecule. Three Au/TiO_2 catalysts are firstly pretreated in O_2 atmosphere at different temperature and then the spectra of CO adsorption on Au/TiO_2 are collected every minute. The experimental results of Au/Ti-100 are presented In **Fig. 3a**. Two peaks corresponding to $Au^{\delta+}$-CO (2110~2120 cm^{-1}) and Au^0-CO (2070~2080 cm^{-1}) can also be observed. Interestingly, as the time prolongs, the intensity of $Au^{\delta+}$-CO gradually goes down and the intensity of Au^0-CO grows up. The transformation of $Au^{\delta+}$ to Au^0 should be caused by the reduction of $Au^{\delta+}$ by CO. When the temperature increase from 250 ^oC to 300 ^oC, the intensity of $Au^{\delta+}$-CO at the beginning stage (0 min) becomes stronger, indicating that O_2 pre-treatment at higher temperature will produce more surface $Au^{\delta+}$ species. However, when the temperature increases to 350 ^oC, the intensities of the CO adsorption peaks decrease dramatically (It should be noted that the scale bar is different in **Fig.** 3a-350 ^oC). As shown in **Fig. 2**, Au NPs will be encapsulated by TiO_2 when Au/TiO_2 catalysts are pretreated with O_2 at 350 ^oC. These TiO_{2-x} shells will prevent the adsorption of CO on Au NPs, which results in weak adsorption of CO.[29,43] The *in situ* DRIFTS results of Au/Ti-101 are shown in **Fig. 3b**. The changing tendencies of these curves are similar with those of Au/Ti-100, which is consistent with the results obtained in activity tests and TEM images. The initial intensities of $Au^{\delta+}$-CO peaks in Au/Ti-100 are stronger than the corresponding peaks in Au/Ti-001(**Fig. 3c**), because there are more $Au^{\delta+}$ species in Au/Ti-100 sample according to *ex situ* XPS. As for Au/Ti-001, the intensity of $Au^{\delta+}$-CO peak at starting stage is much weaker than those of Au/Ti-100 and Au/Ti-101, which is consistent with the low percentages of $Au^{\delta+}$ in *ex situ* XPS. When Au/Ti-001 is pre-treated with O_2 under 350 ^oC, much stronger $Au^{\delta+}$-CO peak can be observed when CO is just pumped in. This change can be well correlated with the sudden increase of $Au^{\delta+}$ percentage in *ex situ* XPS after O_2 pre-treatment at 350 ^oC.

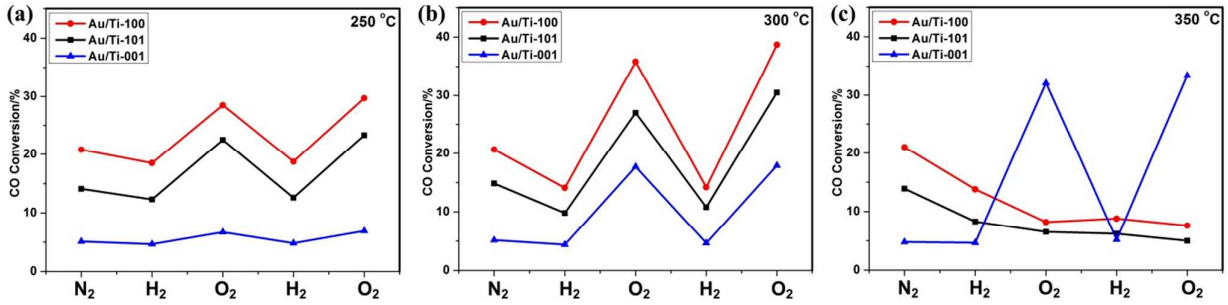

Fig. 4. CO oxidation activities of Au NPs supported on different TiO_2 crystal planes at 30 °C. The catalysts are firstly pretreated under different atmosphere for 1 h at different temperature before testing the CO oxidation activities at 30 °C: (a) 250 °C, (b) 300 °C and (c) 350 °C.

At last, we use H_2 and O_2 to pre-treat three Au/TiO_2 catalysts and employ CO oxidation as probe reaction to investigate the relationships between Au-TiO_2 interaction and the catalytic properties. During the H_2 and O_2 pre-treatments, electrons will transfer across the Au-TiO_2 interface driven by the atmosphere at high temperature. In **Fig. 4**, the CO oxidation activity of Au/TiO_2 catalysts are tested at 30 °C after different pre-treatments at three temperature 250 °C, 300 °C and 350 °C. After the pre-treatments, the sample is kept in reaction steam for 15 min to reach the balance before measure the activity. Obviously, three catalysts show distinct variation tendencies under alternant reductive and oxidative pre-treatments at different temperatures. At 250 °C and 300 °C, for Au/Ti-001, only small changes in activity can be observed, suggesting that Au NPs supported on {001} planes of TiO_2 are not sensitive to the pre-treatments at those conditions. For Au/Ti-101 and Au/Ti-100, the CO conversion will slightly decrease after H_2 pre-treatments at 250 °C and 300 °C because of the weak adsorption of CO. However, an O_2 pre-treatment will remarkably improve the CO conversion of Au/Ti-101 and Au/Ti-100. After O_2 pre-treatment, electrons will flow from Au NPs to TiO_2 supports, resulting in the formation of Ti^{3+} sites around Au NPs.[15] Theoretical study have proved that O_2 activation will be facilitated by the $Au^{\delta+}$-Ti^{3+} structure.[44,45] Thus, activity oscillations can be observed for Au/Ti-101 and Au/Ti-100 when they are pre-treated with H_2 and O_2 before CO oxidation tests, which is similar with their oscillations of $Au^{\delta+}$ percentages. According to our previous work and related references, the percentages of cationic Au species can be well correlated with the CO oxidation activities.[21,24] Therefore, $Au^{\delta+}$ species should be the major active species in CO oxidation in our samples. Notably, Au/Ti-100 shows higher CO conversions than Au/Ti-101 both after H_2 and O_2 treatments, which should be related with their different Au-TiO_2

interface structures as we discussed in our previous work.[24] There are more surface hydroxyl groups on the {100} planes than {101} and {001} planes, which would facilitate the CO oxidation at the Au-TiO_2 interface.[46] But the situation changes when the pre-treatment temperature increases to 350 ^oC. The inert Au/Ti-001 sample shows enhanced CO oxidation activity after O_2 pre-treatment at 350 ^oC, which is in accordance with its increase of $Au^{\delta+}$ percentages. And the activity will fall back after H_2 treatment, which is similar with the behaviours of Au/Ti-100 and Au/Ti-101 when they are pre-treated at 250 ^oC and 300 ^oC. As for Au/Ti-100 and Au/Ti-101, both H_2 and O_2 pre-treatments at 350 ^oC will deactivate the catalysts. The CO conversion decrease to below 10% after O_2 pre-treatment at 350 ^oC. The improvement of O_2 treatment seems ineffective at high temperate for Au/Ti-100 and Au/Ti-101, which is totally different with their variation tendencies at 250 ^oC and 300 ^oC. Combining the above *ex situ* XPS, TEM and *in situ* DRIFTS results, we can infer that the encapsulation of Au NPs should be the reason for the low CO oxidation activities after O_2 pre-treatments at 350 ^oC.[29,43]

According to above analysis based on structural and spectroscopic characterizations and activity measurements, we can have a comprehensive discussion on the crystal-plane-dependent metal-support interaction effects on Au/TiO_2 catalysts. A schematic illustration about the structural changes of three Au/TiO_2 catalysts during pre-treatments under H_2 and O_2 atmosphere at different temperatures are displayed in **Fig. S11**. For Au/Ti-100 and Au/Ti-101, electrons can be flexibly transferred between Au NPs and {100} and {101} planes driven by H_2 and O_2 pre-treatments at 250 ^oC and 300 ^oC. As a result, The percentages of $Au^{\delta+}$ and CO oxidation activities will show oscillations during alternate pre-treatments. For Au/Ti-001, electron-transfer process between Au NPs and {001} facets are not favoured at 250 ^oC and 300 ^oC. No apparent oscillations can be found in the percentages of $Au^{\delta+}$ and CO oxidation activities can be observed. These results show that the metal-support interaction effects are greatly dependent on the crystal planes of TiO_2 supports. The charge-transfer process between Au NPs and TiO_2 supports are affected by the electronic structures of TiO_2. When the pre-treatment temperature increases to 350 ^oC, the situation changes. Much stronger metal-support interaction effects occurred due to the high-temperature pre-treatments. So, the Au-TiO_2 interaction is also related with the temperatures because the electron-transfer processes should be driven by high heating. Apparent oscillations of the percentages of $Au^{\delta+}$ and CO oxidation

activities can be observed in Au/Ti-001 at 350 ^{o}C. However, the Au NPs will be encapsulated by TiO_2 in Au/Ti-100 and Au/Ti-101, leading to the deactivation of Au NPs and disappearance of chemical oscillations. Herein, it should be noted that although we have observed some similar phenomenon like traditional SMSI in Group VIII metals, we still cannot confirm that we have observed SMSI in Au/TiO_2 catalysts.

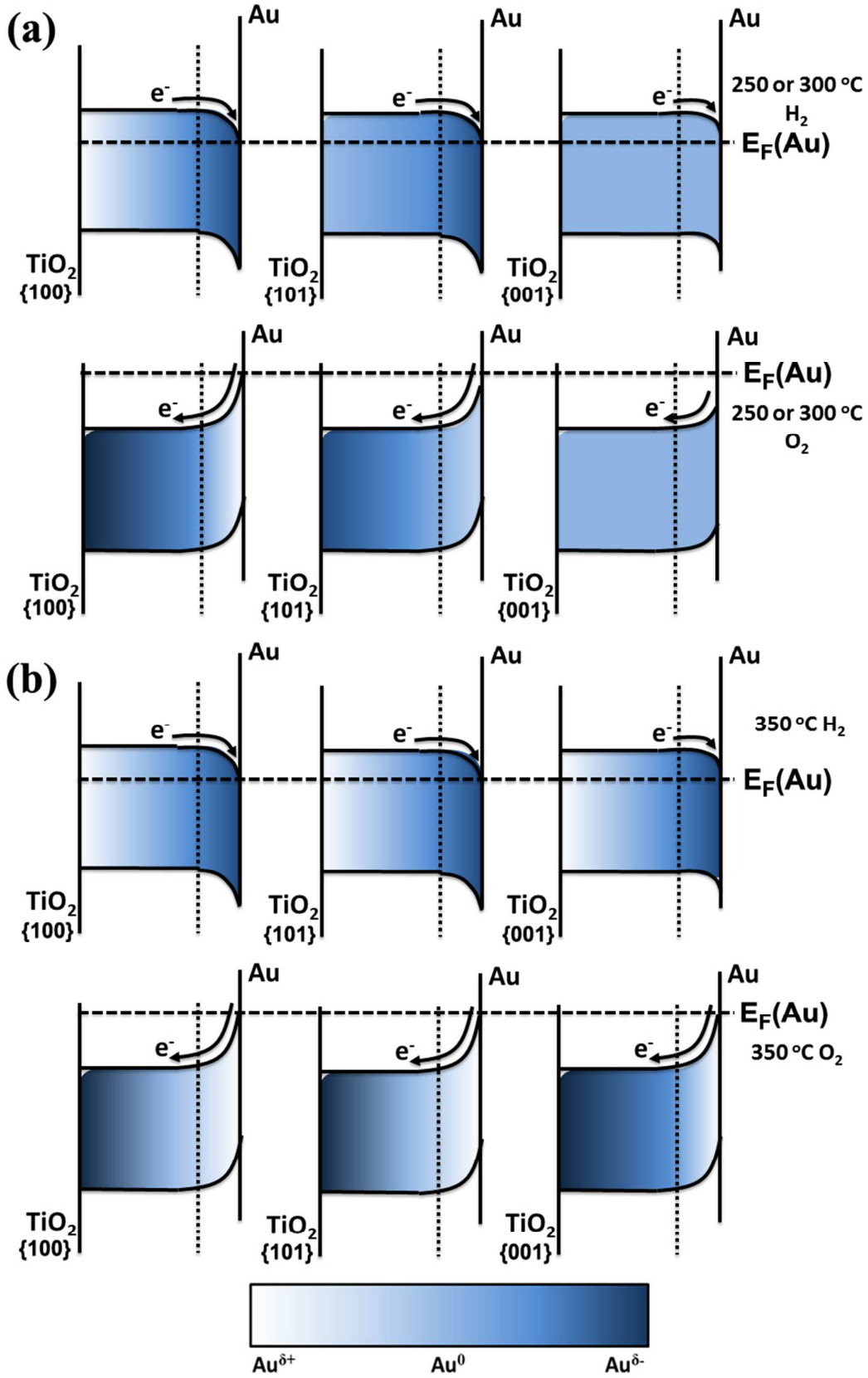

Fig. 5 Schematic illustrations of the band-structure bending and electron flows of different Au-TiO_2

interfaces during the pre-treatments of H_2 and O_2 at different temperatures.

The physiochemical origins of metal-support interaction effects in Au/TiO_2 catalysts are the electron-transfer processes between Au and TiO_2 supports. Band structure diagram of different TiO_2 crystal planes are different according to theoretical calculations and experimental measurements.[23,47] These TiO_2 nanocrystals show the same valence band positions and different conduct band positions. Because of their different band structures, the electronic interactions between Au NPs and different TiO_2 crystal planes under H_2 and O_2 pre-treatments will be distinct with each other. We can use a band energy scheme to demonstrate the changes of electronic structures under H_2 and O_2 pre-treatments. At first, charge equilibriums between Au NPs and TiO_2 nanocrystals with different crystal planes exposed (as shown in **Fig. 5**) after Au NPs are loaded on TiO_2 nanocrystals. When Au/TiO_2 catalysts are exposed to O_2 or H_2, band bending will occur in the Au-TiO_2 heterojunction, leading to electron transfer across the Au-TiO_2 interface.[48,49] When Au/TiO_2 samples are pre-treated with O_2, the Fermi energy of Au NPs (denoted as E_F(Au)) will become higher than that of TiO_2 nanocrystals (denoted as E_F(TiO_2)).[50] The degrees of bending of the energy band (equal to the work function differences between Au NPs and TiO_2 nanocrystals) may be larger between Au NPs and {100} planes and {101} planes than {001} planes, leading to a more favoured electron transfer from Au NPs to TiO_2 nanocrystals.[51] When Au/TiO_2 samples are pre-treated with H_2, E_F(Au) will be lower than E_F(TiO_2), resulting in an opposite electron transfer from TiO_2 nanocrystals to Au NPs.[50] The accumulated electrons in TiO_2 nanocrystals with flow back to Au NPs. As a consequence, chemical oscillations will appear after alternate pre-treatments. At relative low temperature (250 ^oC and 300 ^oC), the more apparent chemical oscillation can be observed in Au/Ti-100 and Au/Ti-101 because of their larger degrees of bending of energy band than Au/Ti-001. At higher temperature (350 ^oC), the degree of bending of energy band in between Au NPs and TiO_2 nanocrystals will become larger. So, apparent chemical oscillations can also be observed in Au/Ti-001. For Au/Ti-100 and Au/Ti-101, driven by high temperature, the Au NPs are encapsulated by TiO_{2-x} shells, leading to the loss of catalytic activities.

In summary, we have studied the crystal-plane-dependent metal-support interactions in Au/TiO_2 using TiO_2 nanocrystals with specific crystal planes exposed as model supports. Using *ex situ* XPS, TEM and *in situ* DRIFTS, we have found that chemical oscillations can be observed during alternate

H_2 and O_2 pre-treatments. These chemical oscillations are greatly dependent on the crystal planes of TiO_2 nanocrystals. As a consequence of these chemical oscillations, their CO oxidation activities also show corresponding variations to the pre-treatments. Considering the discrepancies of different TiO_2 crystal planes in electronic structures, the electronic interactions between Au NPs and TiO_2 nanocrystals will be distinct with each, which should be the origins for their different metal-support interaction effects. However, more works still need to be done to further investigate the crystal-plane effects on metal-support interaction mechanism Au/TiO_2 at a molecular level. Maybe theoretical calculations[52-54] and studies on surface model catalysts[55] will provide some more information. We think this present study will provide some new insights to understand the metal-support interaction effects in Au/TiO_2 and may help to design more active Au/TiO_2 catalysts based on suitable pre-treatments.

Supporting Information

The preparation methods, characterizations and some other related data are shown in supporting information. This material is available free of charge via the Internet at http://pubs.acs.org.

Corresponding Author

gaofei@nju.edu.cn (F.G.)

donglin@nju.edu.cn (L.D.)

Tel.: +86 25 83592290; fax: +86 25 83317761.

Notes

The authors declare no competing financial interests.

Acknowledgement

The financial supports of the National Natural Science Foundation of China (No. 21203091), Natural Science Foundation of Jiangsu Province (BK2012298).

References

1 G. Ertl, H. Knozinger, F. Schuth and J. Weitkamp, *Handbook of Heterogeneous Catalysis*, Wiley-VCH, Weinheim, 2008.

2 G. A. Somorjai and Y. Li, *Introduction to Surface Chemistry and Catalysis*; John Wiley & Sons, Inc.: Hoboken, NJ, 2010.

3 S. J. Tauster, *Acc. Chem. Res.*, 1987, **20**, 389-394.

4 S. J. Tauster, S. C. Fung and R. L. Garten, *J. Am. Chem. Soc.*, 1978, **100**, 170-175.

5 S. J. Tauster, S. C. Fung, R. T. K. Baker and J. A. Horsley, *Science*, 1981, **211**, 1121-1125.

6 Q. Fu and T. Wagner, *Surf. Sci. Rep.*, 2007, **62**, 431-498.

7 L. R. Baker, A. Hervier, H. Seo, G. Kennedy, K. Komvopoulos and G. A. Somorjai, *J. Phys. Chem. C*, 2011, **115**, 16006-16011.

8 E. Gross and G. A. Somorjai, *Topics in Catalysis*, 2013, **56**, 1049-1058.

9 A. S. Hashmi and G. J. Hutchings, *Angew. Chem. Int. Ed.*, 2006, **45**, 7896-7936.

10 Y. Zhang, X. Cui, F. Shi and Y. Deng, *Chem. Rev.*, 2012, **112**, 2467-2505.

11 M. Chen and D. W. Goodman, *Acc. Chem. Res.*, 2006, **39**, 739-746.

12 J. Gong, *Chem. Rev.*, 2012, **112**, 2987-3054.

13 D. W. Goodman, *Catal. Lett.*, 2005, **99**, 1-4.

14 Y. Kuwauchi, H. Yoshida, T. Akita, M. Haruta and S. Takeda, *Angew. Chem. Int. Ed.*, 2012, **51**, 7729-7733.

15 T. Tanaka, K. Sano, M. Ando, A. Sumiya, H. Sawada, F. Hosokawa, E. Okunishi, Y. Kondo and K. Takayanagi, *Surf. Sci.*, 2010, **604**, L75-L78.

16 W. Jochum, D. Eder, G. Kaltenhauser and R. Kramer, *Top. Catal.*, 2007, **46**, 49-55.

17 Q. Fu, W. X. Li, Y. Yao, H. Liu, H. Y. Su, D. Ma, X. K. Gu, L. Chen, Z. Wang, H. Zhang, B. Wang and X. Bao, *Science*, 2010, **328**, 1141-1144.

18 J. A. Rodriguez, S. Ma, P. Liu, J. Hrbek, J. Evans and M. Perez, *Science*, 2007, **318**, 1757-1760.

19 Z. Zhong, J. Ho, J. Teo, S. Shen and A. Gedanken, *Chem. Mater.*, 2007, **19**, 4776-4782.

20 L. C. Wang, Y. M. Liu, M. Chen, Y. Cao, H. Y. He and K. N. Fan, *J. Phys. Chem. C*, 2008, **112**, 6981-6987.

21 R. Si and M. Flytzani-Stephanopoulos, *Angew. Chem. Int. Ed.*, 2008, **47**, 2884-2887.

22 G. Liu, J. C. Yu, G. Q. Lu and H. M. Cheng, *Chem. Commun.*, 2011, **47**, 6763-6783.

23 L. Liu, X. Gu, Z. Ji, W. Zou, C. Tang, F. Gao and L. Dong, *J. Phys. Chem. C*, 2013, **117**, 18578-18587.

24 L. Liu, X. Gu, Y. Cao, X. Yao, L. Zhang, C. Tang, F. Gao and L. Dong, *ACS Catal.*, 2013, **3**, 2768-2775.

25 L. Qi, C. Tang, L. Zhang, X. Yao, Y. Cao, L. Liu, F. Gao, L. Dong and Y. Chen, *Appl. Catal. B: Environ.*, 2012, **127**, 234-245.

26 R., Meyer, C. Lemire, S. K. Shaikhutdinov and H.-J. Freund, *Gold Bull.* 2004, **37**, 72-124.

27 Z. Jiang, W. Zhang, L. Jin, X. Yang, F. Xu, J. Zhu and W. Huang, *J. Phys. Chem. C*, 2007, **111**, 12434-12439.

28 D. Matthey, J. G. Wang, S. Wendt, J. Matthiesen, R. Schaub, E. Laegsgaard, B. Hammer and F. Besenbacher, *Science*, 2007, **315**, 1692-1696.

29 X. Liu, M. H. Liu, Y. C. Luo, C. Y. Mou, S. D. Lin, H. Cheng, J. M. Chen, J. F. Lee and T. S. Lin, *J. Am. Chem. Soc.*, 2012, **134**, 10251-10258.

30 V. A. O'Shea, M. C. Galvan, A. E. Prats, J. M. Campos-Martin and J. L. Fierro, *Chem. Commun.*, 2011, **47**, 7131-7133.

31 S. Bernal, J. J. Calvino, M. A. Cauqui, J. M. Gatica, C. López Cartes, J. A. Pérez Omil and J. M. Pintado, *Catal. Today*, 2003, **77**, 385-406.

32 H. Iddir, S. Öğüt, N. Browning and M. Disko, *Phys. Rev. B*, 2005, 72.

33 H. Onishi and Y. Iwasawa, *Surf. Sci.,* 1994, **313**, L783-L789.

34 P. Stone, R. A. Bennett and M. Bowker, *New J. Phys.* 1999, **1**, 1.1-1.12.

35 H. Yin, Z. Ma, H. Zhu, M. Chi and S. Dai, *Appl. Catal. A: Gen.*, 2010, **386**, 147-156.

36 G. W. Graham, A. E. O'Neill and A. E. Chen, *Appl. Catal. A: Gen.*, 2003, **252**, 437-445.

37 G. W. Graham, H.-W. Jen, W. Chun and R. W. McCabe, *J. Catal.* 1999, **182**, 228-233.

38 L. Li, A. Wang, B. Qiao, J. Lin, Y. Huang, X. Wang and T. Zhang, *Journal of Catalysis*, 2013, **299**, 90-100.

39 M. Mihaylov, E. Ivanova, Y. Hao, K. Hadjiivanov, H. Knözinger and B. C. Gates, *J. Phys. Chem. C*, 2008, **112**, 18973-18983.

40 M. Mihaylov, H. Knozinger, K. Hadjiivanov and B. C. Gates, *Chem. Ing. Tech.* 2007, **79**,

795-806.

41 F. Boccuzzi, A. Chiorino, M. Manzoli, D. Andreeva and T. Tabakova, *J. Catal.*, 1999, **188**, 176-185.

42 F. Boccuzzi, A. Chiorino and M. Manzoli, *Surf. Sci.*, 2000, **454-456**, 942-946.

43 S. Bonanni, K. Aït-Mansour, H. Brune and W. Harbich, *ACS Catal.*, 2011, **1**, 385-389.

44 Y. G. Wang, Y. Yoon, V. A. Glezakou, J. Li and R. Rousseau, *J. Am. Chem. Soc.*, 2013, **135**, 10673-10683.

45 Y. F. Li and A. Selloni, *J. Am. Chem. Soc.*, 2013, **135**, 9195-9199.

46 J. Saavedra, H. A. Doan, C. J. Pursell, L. C. Grabow and B. D. Chandler, *Science*, **2014**, 345, 1599-1602.

47 J. Lu, Y. Dai, H. Jin and B. Huang, *Phys. Chem. Chem. Phys.*, 2011, **13**, 18063-18068.

48 N. Cabrera, N. F. Mott, *Rep. Prog. Phys.* **1949**, *12*, 163-184.

49 A. Motayed and S. N. Mohammad, *J. Chem. Phys.*, 2005, **123**, 194703.

50 P. B. Weisz, *J. Chem. Phys.* 1953, **21**, 1531.

51 Z. Zhang and J. T. Yates, Jr., *J Am Chem Soc*, 2010, **132**, 12804-12807.

52 I. X. Green, W. Tang, M. Neurock and J. T. Yates, Jr., *Science*, 2011, **333**, 736-739.

53 M. Farnesi Camellone and D. Marx, *J. Phys. Chem. Lett.*, 2013, **4**, 514-518.

54 P. Ganesh, P. R. C. Kent and G. M. Veith, *J. Phys. Chem. Lett.*, 2011, **2**, 2918-2924.

55 F. Gao and D. W. Goodman, *Annu. Rev. Phys. Chem.*, 2012, **63**, 265-286.